A Study on Reciprocity Law Failure using Human Phantoms in Digital Radiography

[1]Hyeong-Gyun Kim

Abstract: Background/Objectives: The purpose of this study was to analyze the subject images of the human body Phantom under the X-ray exposure condition of the DR system and to confirm the reciprocity law and the reciprocity law failure phenomenon of the soft tissues and bone tissues. Methods/Statistical analysis: After adjusting the tube current-exposure time product (mAs) to the same value, the reciprocity law was confirmed by averaging the pixel gray values at a certain position from X-rays of 3 different exposure conditions changing the tube current (mA) and exposure time (sec). Image analysis was performed using the grid and plot profile functions of the image J program to compare the reciprocity law in the thickness between the soft tissues and bone tissues. Findings: As a result, large reciprocity law failures were observed in the low bone thickness area of the foot phantom and the soft tissues with low tissue density, and the same results were found in the experiment using the abdomen phantom which has a high subject thickness. Improvements/Applications: As a result, this study confirmed that reciprocity law and reciprocity failure due to X-ray exposure may occur between human tissues in adjacent areas.

Keywords: DR (digital radiography), Reciprocity law failure, Phantom, Tube current amount (mAs), image

I. INTRODUCTION

After X-rays were discovered by Roentgen in 1895, the radiological X-ray equipment for human diagnosis has developed into the CR (computed radiography) and DR (digital radiography) system through a Film system that records images with chemical development processing[1,2]. However, in current clinical trials, DR equipment is widely used to diagnose human bodies by X-ray. Such DR (Digital Radiography) refers to CT (Computed Tomography), MRI (Magnetic Resonance Imaging), USG (Ultra Sonography), and fluoroscopic equipment that acquire digital images in a broad sense, but in a general narrow sense, DR refers to the digitization of a simple general radiography and refers to the system subject to this study[3,4]. Thus, in the case of general radiography, the same image diagnostic results of the same aspect are obtained, although the method of acquiring the image differs between the film of the past and the current DR method[5-7]. Therefore, this study was performed to investigate the relationship between the reciprocity law failure that applies to the Film system and the DR method[8]. The reciprocity law was first applied in general photography, stating that the amount of exposure is proportional to the product of exposure intensity and exposure time. In general radiography, the reciprocity law refers to when the tube voltage (kVp) is equal to the tube current amount (mAs), the photographic density of the image is the same even if the ratio of tube current (mA) and exposure time (sec) varies[9]. However, when either the exposure intensity or exposure time becomes an extreme value, reciprocity law failure occurs[10]. Based on these literature technologies, this study intends to examine reciprocity failure on the subject by experimenting with different variables of thickness and density of the human phantom in the latest X-ray digital equipment. Since the influence factors such as tube current (mA) and exposure time (sec) can be changed randomly during radiography X-ray imaging, this study established experimental conditions to examine the relationship of reciprocity failure.

II. MATERIALS AND METHODS

2.1 Experimental equipment and materials

This study used TITAN 2000 (TOSHIBA, JAPAN) digital X-ray equipment and acrylic foot and pelvis phantom[Figure 1]. The Image J program was used to measure the change in the region of interest (ROI)[11,12], and the Grid function of the program was used to measure the pixel value of the image density by measuring the same area that was uniformly divided.

The diagnostic X-ray imaging equipment(a) and the human foot phantom(b) used in the experiment.

Figure 1. The diagnostic X-ray equipment and foot phantom used in the experiment

2.2 Experimental method

The experiment was performed by fixing the source to surface distance (SSD) of the foot phantom subject at 100 cm, and aligning the center line to the 3rd phalanges and metatarsal as the foot phantom AP (anterior-posterior) projection position. Based on the default values of the equipment, the exposure condition acquired foot images of test 1, 2, and 3 in 3 phases by changing the tube current (mA) and exposure time (sec). In terms of the detailed exposure condition, after adjusting the tube voltage to 55 kVp and the tube current amount to 8 mAs, the average pixel value of the images were recorded by increasing the tube current to 100 mA, 200 mA, and 400 mA and changing the exposure time in the order of 0.08 sec, 0.04 sec, and 0.02 sec[Table 1]. Considering the heel effect, the proximal side of the human body was positioned as the cathode of the X-ray tube and the toe side as the anode for imaging. The ROI measurement was performed by setting 9 points on the foot image using the Grid function of Image J to obtain the pixel values. As shown in Figure 2,

Revised Manuscript Received on January 03, 2019.

Hyeong-Gyun Kim , Corresponding author, Dept. of Radiology Science, Far East University, Chungbuk, Korea.

after setting points 1, 2, and 3 as the upper end, points 4, 5, and 6 as the middle, and points 7, 8, and 9 as the bottom end, the pixel value of each point was obtained[Figure 2. a]. The measurements were taken three times under the same exposure condition to obtain the average value. In order to confirm the position of the human body, the measurements were taken after enlarging the images to distinguish the bones and the soft tissues[Figure 2. b, c]. This process was then compared to the pixel value of each point using the point mark function of the image J program. In addition, after setting areas with the same bone density in the foot image, the relative differences were compared by the graphs made by the plot profile of the image J program[Figure 3].

Table 1: Experiment exposure conditions

	test 1	test 2	test 3
kVp	55	55	55
mAs	8	8	8
mA	100	200	400
Sec	0.08	0.04	0.02

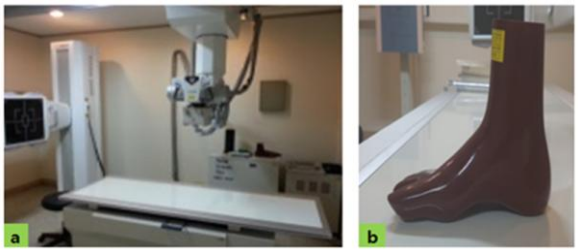

The 9 measurement points(a) and enlarged image of the bones and soft tissues(b) are shown using the grid function.

Figure 2. The pixel value measurement positions in the foot phantom
image

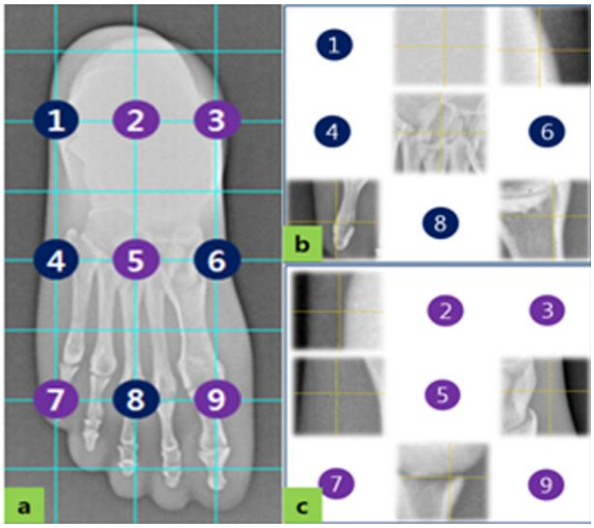

Shows the gray value plot profile(a) graph of the setting position(red line in Figure b).

Figure 3. Bone measurement positions with the same density in the foot phantom images

III. MATH

3.1 Change of reciprocity law in foot phantom images

From the images acquired with the test 1, 2, and 3 conditions for the foot phantom, [Table 2] shows the average values of the pixel gray values at each of the preset positions by the experimental method. The reciprocity law for the same tube current amount was different in the bone and soft tissues. Test 1 and test 3 showed values of 873, 1794, 1724, 5290 and 3523 in 2, 3, 5, 7 and 9, respectively, where bone tissues are heavily distributed. For 1, 4, 6, and 8, where the soft tissues are distributed, the values were 15861, 10862, 6270, and 12572, indicating that the difference in the average value of variation was higher than that of the bone tissue[Table 3] [Figure 4].

Table 2: Average gray value according to the pixel position in the foot phantom

Position Number	1	2	3	4	5	6	7	8	9
test 1	26467	52303	58608	33282	48140	40788	46064	28716	48055
test 2	37378	51509	57639	41232	49882	46374	49811	37386	52013
test 3	42328	51430	56814	44144	49864	47058	51354	41288	51578

Table 3: Absolute value difference of average gray value according to foot phantom pixel position

Position Number	1	2	3	4	5	6	7	8	9
test 1 - test 2	10911	794	969	7950	1742	5586	3747	8670	3958
test 1 - test 3	15861	873	1794	10862	1724	6270	5290	12572	3523
test 2 - test 3	4950	79	825	2912	18	684	1543	3902	3435

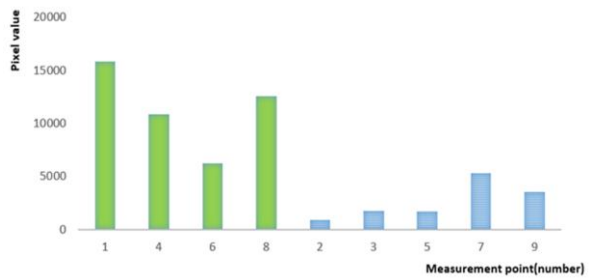

The horizontal axis shows the measured positions 1, 4, 6, and 8 of the soft tissues and 2, 3, 5, 7, and 9 of the bone tissues.

Figure 4. The reciprocity failure comparison graph in the soft and bone tissues under test 1 and 3 conditions

3.2 Change of reciprocity law in bones with the same density

In order to examine the value of change for bone tissues in which the reciprocity

law applies relatively better than the soft tissues, using the Plot Profile function of Image J, the longitudinal sagittal lines of 2, 5, and 8 were merged into a graph corresponding to each condition of test 1, 2, and 3[Figure 5]. As shown in Figure 5, (a) indicates the tarsals bone of the Calcaneus and talus, (b) the tarsometatarsal joint, and (c) the metatarsal bone, and the positions are divided into three parts of a certain interval. As a result, the average value of the change in pixel value in the direction of the toe with increasingly thinner bone tissue was higher[Figure 5].

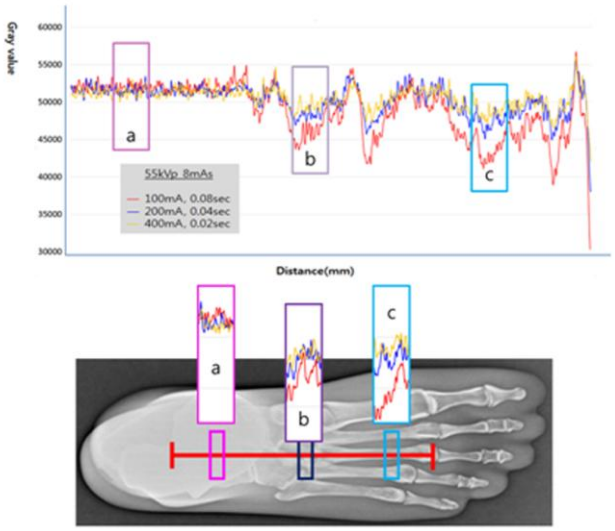

The three parts in the toe direction of the tarsals of the Calcaneus and talus(a), tarsometatarsal joint(b), and metatarsal(c) are shown at regular intervals.

Figure 5. The reciprocity failure plot profile graph of the bone tissue

IV. DISCUSSION

In order to identify the influence factors of the reciprocity law failure, a foot phantom was used to examine the reciprocity law phenomenon in five bone tissues and four soft tissues. The foot phantom used in the experiment due to the characteristics of human anatomy, as it is a mixture of soft tissue and bone tissue with a large difference in the thickness of the subject[13]. However, since one phantom limits the reliability of the measured value, this study carried out the process of adding experiments with an abdomen phantom, which is rich in bone and soft tissues[Figure 6]. As shown in Figure 6, the measurement results of the 9 points using the grid function of image J are similar to those of the reciprocity law from the foot. That is, as 1, 4, and 7 leading to line (a) and 1, 5, and 9 of line (b) are the soft tissue, overlapping area of the partial volume effect[14], and where the bone tissue continues, the average value of change in the soft tissue was higher than that of the bone tissue[Table 4].

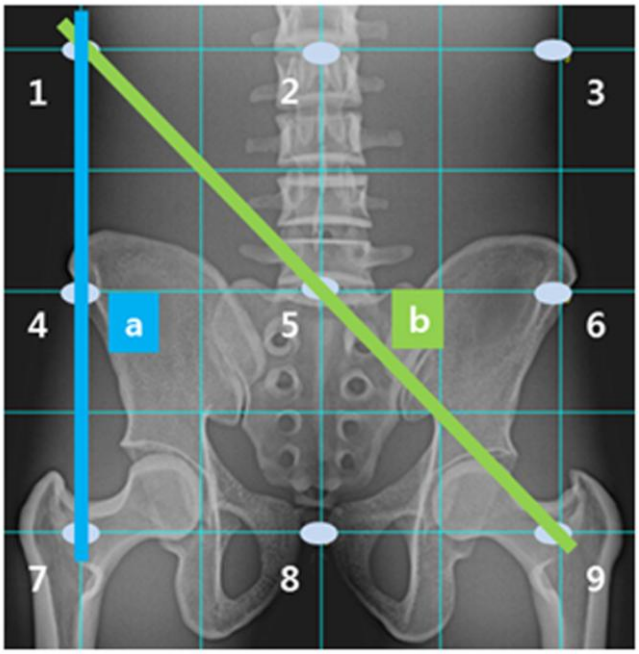

In the figure, line (a) shows the position of 1, 4, and 7, and line (b) the position of 1, 5, and9, respectively.

Figure 6. Abdomen phantom image measurement location

Table 4: Average value of change according to the pixel position in the abdominal phantom

position	1	2	3	4	5	6	7	8	9
average value	46275	18532	46216	31568	30399	30682	26967	36217	27008

As the image acquisition principle used in this study is DR (digital radiography), the images were not acquired by creating latent images using the principle of photography (photosensitivity) of film, but by computerizing the radiation received from the detector and then transferring them to a computer to reconstruct them into images[15-17]. The images obtained are displayed by acquiring the pixel value of a specific point using the Image J program which is capable of expressing in pixel values. As a result, this study examined the effects of the density difference between the soft tissue and bone tissue as well as the effect of the thickness of the subject on the reciprocity law failure phenomenon with the Plot Profile function. Thus, the clinical use of DR systems should also consider the reciprocity law failure, and short exposure time examinations of emergency or pediatric patients should consider the technical circumstances that may lead to reciprocity failure.

V. CONCLUSION

From the foot images acquired by changing the condition to the same tube current amount (mAs) in diagnostic X-ray imaging using DR equipment, the average value of pixel gray value change, shown by density and thickness differences, showed relatively high reciprocity failure phenomenon in the low-density soft tissue and areas with low bone thickness. As a result, this study confirmed that there is also a difference in reciprocity law failure among human tissues in the

same location.

REFERENCES

1. Floyd C E , Warp R J , Dobbins J T , Chotas H G , Baydush A H , Vargas-Voracek R , et al. Imaging Characteristics of an Amorphous silicon Flat-Panel Detector for Digital Chest Radiography. Radiology. 2001;218: 683-88.
2. Radiation Control Textbook Compilation Committee: Radiation Protection & Safety. Chung-Ku; 2014.
3. Seong-gyu Shin, Hyo-Yeong Lee. The Anode Heel Effect caused by changing the Angle of X-Ray Tube. Journal Korean Society Radiology. 2016;10(6):435-42.
4. Research Association a medical image information system, PACS for Medical Image. Chung-Ku; 2014.
5. Harrell G. Chotas, Carl E. Ravin. Digital Chest Radiography with a Solid-state Flat-Panel X-ray Detector: contrast-Detail Evaluation with Processed Images Printed on Film Hard Copy. Radiology. 2001;218:679-82.
6. Byeongju An. A comparative study for resolution and density of chest imaging using film/screen, CR and DR. Journal of the Korean Society of Radiology. 2010;4(1): 25-30.
7. Marietta Garmer, Svenja P. Hennigs, Horst J. Jager, et al. Digital Radiography Versus Conventional Radiography in Chest Imaging: Diagnostic Performance of a Large-Area Silicon Flat-Panel Detector in a Clinical CT-Controlled Study. AJR. 2000;174:75-80.
8. Bo Ra Kim, Sin Young Ryu, Jin Young Seok, Jun Gu Choi. Analysis of Original and Processing Image by Control of Exposure Dose, kVp in Digital Radiography. Korean J Digit Imaging Med. 2011;13(1):49-53.
9. Choi Jong Hak. Analog radiographic imaging. Shinkwang pub; 2013.
10. https://terms.naver.com/entry.nhn?docId=786419&cid=42431&categoryId=42431
11. Hongmoon Jung, Doyeon Won, Jaeeun Jung. Quantitative Analysis Methods for Adapting Image J programs on Mouse Calvarial defected Model. The Journal of digital policy & management. 2013;11(9):365–70.
12. Won-Joo Seo, Jeong-Beom Seo, Jong-Woong Lee. Using Image J program, compared of focusing distance and grid rate. Korean journal of digital imaging in medicine. 2012;14(1):37-42.
13. K. J. Jang, N. H. Kim, J. H. Lee, S. B. Lee. Distribution of X-ray Strength in Exposure Field Caused by Heel Effect. Journal of the Korean Society of Radiology. 2011;5(5):223-29.
14. Minju Park, Sangbock Lee. Implementation of Filter for the Removal of Partial Volume Effect. Journal of the Korean Society of Radiology.2015;9(3):139-45.
15. Seon-Chil Kim, Jaeeun Jung. Study on image quality and dosage comparison of F/S system and DR system. Journal of Korean Society of radiological technology. 2003;26(3): 7-11.
16. Veno E, Faulkner KA, Colin GO. Major advantage of medical imaging for general radiograpy is the potential for reduced patient dose so film/screen systems should be phased out as unnecessarily hazardous. Med Phys. 2006;33:1529-31.
17. SC. Kim, JE. Jung. Study on image quality and dosage comparison of F/S system and DR system. Journal of Korean Society of radiological technology. 2003; 26:7-11.